ЯДЕРНА ФІЗИКА
NUCLEAR PHYSICS

УДК 539.12 https://doi.org/10.15407/jnpae2024.03.241

A. Ya. Dzyublik*, I. E. Anokhin, V. Yu. Spivak

Institute for Nuclear Research, National Academy of Sciences of Ukraine, Kyiv, Ukraine

*Corresponding author: dzyublik@ukr.net

ROLE OF BROWNIAN MOTION AND NÉEL RELAXATIONS IN MÖSSBAUER SPECTRA OF MAGNETIC LIQUIDS

The absorption cross-section of Mössbauer radiation in magnetic liquids is calculated, taking into consideration both translational and rotational Brownian motion of magnetic nanoparticles as well as stochastic reversals of their magnetization in the absence of an external magnetic field. The role of Brownian motion in ferrofluids is considered in the framework of the diffusion theory, while for the magnetorheological fluids with large nanoparticles, it is done with the aid of Langevin's approach. For stochastic rotation, we derived the equation analogous to Langevin's one and found the corresponding correlation function. In both cases, simple rotational correlation functions are obtained in the approximation of small rotations during the lifetime of the excited Mössbauer nuclei. Influence of the Néel's relaxations is considered in the framework of the Blume - Tjon model.

Keywords: Mössbauer effect, ferromagnetic nanoparticles, Brownian motion, Néel relaxations.

1. Introduction

Suspensions of magnetic nanoparticles (MNPs) attract great attention due to their numerous applications in technique, medicine, and biology [1 - 17]. It is provided by the large magnetic moment of MNPs, which allows to manipulate them by moderate magnetic fields. Depending on the dimensions of MNPs, they can be divided into magnetorheological fluids formed by MNPs with a diameter of the order of 1 μm and ferrofluids with dimensions of MNPs $\sim$10 nm (see, e.g., [3]). When the magnetorheological liquids are subjected to the magnetic field, their viscosity enormously increases, so that these liquids may even transform into a solid body. This property gives the possibility to use such suspensions in dampers, brakes, and clutches [4].

Ferrofluids are widely used in computers, loudspeakers, semiconductors, motion controllers, sensors, ink-jet printers, seals, bearings, stepper motors, etc. [1 - 8].

In medicine, ferrofluids are employed in hyperthermia [9], for drug delivery to local ill regions of the body, and as contrast agents in magnetic resonance imaging (MRI) [10]. Recently, a much more progressive method of magnetic particle imaging (MPI) was developed for visualizing MNPs in humans and animals [11 - 15]. The advantage of MPI is that it is more fast, quantitative, and sensitive than MRI.

Note that MNPs are always coated with a polymer shell to prevent their agglomeration in a solution. The commercial ferrofluids are predominantly based on magnetite Fe_3O_4 particles.

Usually, MNPs have a single easy-magnetization axis ζ and their magnetization $\mathbf{M}$ tends to be oriented along it or in the opposite direction, keeping the constant value $|\mathbf{M}|$ The anisotropy potential energy of such particles in the absence of external magnetic fields, versus the angle Θ between $\mathbf{M}$ and axis ζ is represented by two potential wells at $\Theta = 0$ and π separated by the potential barrier:

$$E = K_{eff} V \sin^2 \Theta, \qquad (1)$$

where K_{eff} denotes the effective magnetic anisotropy, V the particle volume. The magnetization, oscillating in one of the potential wells, from time to time gets sufficient energy to jump over the barrier into the neighboring well. In the symmetric potential (1) the magnetization reversals occur with equal rates $w = 1/\tau_N$ on both sides, where the relaxation time τ_N is determined by Néel's formula [16]

$$\tau_N = \tau_0 \exp\left(\frac{K_{eff} V}{kT}\right) \qquad (2)$$

with the constant factor $\tau_0 \sim 10^{-9} - 10^{-13} s^{-1}$ (see, e.g., [17]).

The effectiveness of the MNPs in different applications strongly depends on such parameters as the Nèel relaxation time and Brownian rotational relaxation time of MNPs, dependent on the temperature and viscosity of the carrier fluid. The Mössbauer spectroscopy is the most powerful method to

determine such characteristics. Soon after the discovery, the Mössbauer effect was applied for the investigation of the Brownian motion of nanoparticles in liquids [18 - 26]. The foundation of these studies has been laid by Singwi and Sjölander [25], who expressed the absorption cross-section of Mössbauer rays by chaotically moving nanoparticles in terms of the Van Hove auto-correlation function. Having described the translational motion of the Brownian particle by diffusion equation, they found that the broadening of the Mössbauer line linearly depends on the ratio of temperature T and viscosity of the liquid η. This conclusion was supported experimentally for small nanoparticles [18 - 24]. But somewhat later for large particles it was observed considerable curvature of the line, which was explained theoretically in Refs. [23, 24], where the Brownian motion was described by means of the stochastic Langevin's equation.

For the first time, the effect of the Brownian rotation on the shape of the Mössbauer line was analyzed by Zatovskiĭ [26], who found the most strict solution for the absorption cross-section. In Ref. [27] this task has been solved in small-angle approximation, taking into account that during the lifetime of the excited Mössbauer nucleus, the root-mean-square angle of the Brownian rotation is usually much less than unity. Such simple calculations were expanded to the case of ellipsoidal Brownian particles in Ref. [28]. Another somewhat more cumbersome approach to the problem of Brownian rotation has been developed in Ref. [29].

Previously some aspects of Mössbauer spectra of ferrofluids were studied in the theoretical paper [30], whereas Landers et al. [17] seem to be the first who observed the Mössbauer spectra in ferrofluids. Interesting experimental results have been also reported in Refs. [31 - 34].

In this paper, we research in much more detail the impact of Brownian rotation together with translational diffusion on the shape of Mössbauer spectra of MNPs. In particular, for the first time, the Brownian rotation of large nanoparticles is regarded by utilizing Langevin's formalism in full analogy with the translational motion.

For ferrofluids, we shall apply a simplest model of the Nèel relaxations, when the magnetization vector of the particle $\mathbf{M}(t)$ makes stochastic jumps between the values $\mathbf{M}$ and $-\mathbf{M}$ along the easy axis ζ. Respectively, the magnetic field at the nucleus, being antiparallel to $\mathbf{M}(t)$, takes the values $\mathbf{h}_0(t) = \mathbf{h}_0 f(t)$ with $f(t) = \pm 1$. The magnetic field $\mathbf{h}_0$ causes the splitting of the nuclear sublevels giving rise to a Zeeman sextet. Throughout the paper, we suppose that there is no external magnetic field as well there is no interaction between MNPs so that jumps of the magnetization proceed with equal probability in both directions. For generality, we adopt that along the field $\mathbf{h}_0$ there is an electric field gradient, which ensures a quadrupole splitting of the lines. This model was previously applied to calculations of Mössbauer spectra by Blume and Tjon [35].

2. Basic equations

In order to separate the translational and rotational motion we first introduce the coordinate frame x, y, z with the origin in the center of the particle and axis z along the beam of incident γ-quanta. In addition, we introduce the frame ξ, η, ζ with an axis ζ along the easy-magnetization axis of the particle. The position of the Mössbauer nucleus ^{57}Fe in the laboratory frame x_L, y_L, z_L is determined by the radius-vector

$$\mathbf{X} = \mathbf{R} + \mathbf{r} + \mathbf{u}, \tag{3}$$

where the vector $\mathbf{R}$ indicates the position of the center of the Brownian particle, $\mathbf{r}$ specifies the equilibrium position of the nucleus in the frame x, y, z, and $\mathbf{u}$ is the displacement from this site (Fig. 1).

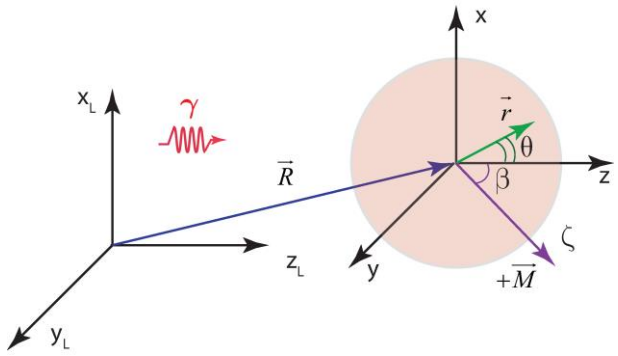

Fig. 1. Scheme illustrating motion of the Mössbauer nucleus ^{57}Fe together with the spherical Brownian particle, whose easy-magnetization axis is labeled by ζ. The vector **R** indicates the position of this particle in the laboratory frame, **r** the equilibrium position of the nucleus inside the particle. (See color Figure on the journal website.)

Random reversals of the magnetization **M** and the Brownian motion are independent processes. Therefore the absorption cross-section of γ-quanta with the energy $E = \hbar\omega$ and wave vector $\boldsymbol{\kappa}$ by the Mössbauer nucleus ^{57}Fe, embedded in the Brownian particle, may be written as [30]

$$\sigma_a(\omega) = \frac{\sigma_0 \Gamma_a}{2} e^{-2W_a} \times$$

$$\times Re\int_0^\infty \frac{dt}{\hbar} e^{i(\omega-\omega_a)t-\Gamma_a t/2\hbar} G_B(\boldsymbol{\kappa},t) G_N(\boldsymbol{\kappa},t), \quad (4)$$

where σ_0 is the resonant value of the absorption cross-section of γ-quanta by a fixed nucleus in the absence of the hyperfine structure, $E_a = \hbar\omega_a$ and Γ_a are the energy and width of the resonant level of the absorbing nucleus, e^{-2W_a} is the Debye - Waller factor, $G_B(\boldsymbol{\kappa},t)$ denotes the Fourier-transform of the classical self-correlation function for the Brownian motion, $G_N(\boldsymbol{\kappa},t)$ the correlation function for the Néel relaxations of magnetization.

This cross-section is to be averaged over the energy distribution of γ-quanta emitted by a source without recoil

$$w_e(E) = \frac{\Gamma_e}{2\pi} \frac{1}{(E-E_e-s)^2 + (\Gamma_e/2)^2}, \quad (5)$$

where $s = vE_e/c$ denotes the Doppler shift for a source, moving with the velocity v relative to an absorber. Then if $E_e = E_a$ experimentally measured cross-section takes the form

$$\sigma_a(s) = \frac{\sigma_0\Gamma_a}{2} e^{-2W_a} \times$$

$$\times Re\int_0^\infty \frac{dt}{\hbar} e^{ist/\hbar - \Gamma_0 t/2\hbar} G_B(\boldsymbol{\kappa},t) G_N(\boldsymbol{\kappa},t), \quad (6)$$

where $\Gamma_0 = \Gamma_e + \Gamma_a$ means the width observed when any broadening due to Brownian motion or Néel relaxations is absent.

For spherical particles the translational and rotational Brownian motions are separated, so that

$$G_B(\boldsymbol{\kappa},t) = G_s^t(\boldsymbol{\kappa},t) G_s^r(\boldsymbol{\kappa},t), \quad (7)$$

where $G_s^t(\boldsymbol{\kappa},t)$ and $G_s^r(\boldsymbol{\kappa},t)$ are the Fourier transforms of the self-correlation functions for translational motion and rotation, respectively.

3. Correlation functions

In this section, we shall give the correlation functions for the translational and rotational Brownian motion of spherical nanoparticles in a liquid, provided by corresponding diffusion equations. Besides, the correlator responsible for the Néel relaxations of the MNPs magnetization, derived in Ref. [35], will be reproduced below in a somewhat changed form.

3.1. Translational Brownian motion

For the translational Brownian motion, described by a simple diffusion equation, the self-correlation function has the form [25]

$$G_s^t(\mathbf{R},t) = (4\pi D_t |t|)^{-3/2} \exp[-R^2/4D_t|t|]. \quad (8)$$

Here we suppose that at the initial moment, $t = 0$ the particle is located in the origin of the laboratory frame. The Fourier transform of the function (8) reads

$$G_s^t(\boldsymbol{\kappa},t) = \exp(-\kappa^2 D_t |t|). \quad (9)$$

By using this equation Singwi and Sjolander [25] found that the Mössbauer line is described by the Lorentzian curve having the width

$$\Gamma = \Gamma_0 + \Delta\Gamma_t, \quad (10)$$

where the line broadening is related to the translational diffusion coefficient D_t by

$$\Delta\Gamma_t = 2\hbar\kappa^2 D_t. \quad (11)$$

For spherical particles

$$D_t = \frac{kT}{6\pi\eta a_h}, \quad (12)$$

where T and η denote the temperature and viscosity coefficient of the liquid, a_h the hydrodynamic radius of the nanoparticle, which equals the sum of the core radius a_c and the thickness of its polymer coating d.

3.2. Brownian rotation

The mean-square angle of rotation Δ_r^2 of the Brownian particle in a liquid during time t is determined by Einstein's formula [36]

$$\Delta_r^2 = 2D_r t, \quad (13)$$

depending on the rotation diffusion coefficient

$$D_r = \frac{kT}{8\pi\eta a_h^3}, \quad (14)$$

where a_h is the hydrodynamic radius of the particle.

Let us estimate the Δ_r^2 for rotation during the time t of the order of the lifetime $\tau_N = \hbar/\Gamma_a = 141$ ns for ^{57}Fe. We take the parameters of the experiment [17], which correspond to maximal value of Δ_r^2: $a_h = 7$ nm and $\eta = 22.5$ cp (viscosity of the 70 % glycerol solution at $T = 293$ K). In this case $\Delta_r^2 \approx 4\cdot10^{-3}$. In all other measurements [17], corresponding to lower tempera-

tures and larger particles Δ_r^2 is much less. Thus, we can really treat the Brownian rotation in the small-angle approximation.

The Fourier-transform of the rotational correlation function is calculated with the aid of the probability density $G_s^r(\mathbf{n},\mathbf{n}_0;t)$ of the Brownian rotation from $\mathbf{n}_0$ to $\mathbf{n}$ during time t:

$$G_s^r(\boldsymbol{\kappa},t)=\int d\mathbf{n}G_s^r(\mathbf{n},\mathbf{n}_0;t)e^{i\boldsymbol{\kappa}(\mathbf{n}-\mathbf{n}_0)r}, \qquad (15)$$

where orientation of the unit vectors $\mathbf{n}_0=\mathbf{r}(0)/r$ and $\mathbf{n}=\mathbf{r}(t)/r$ in the frame x, y, z are determined by the spherical angles θ_0,ϕ_0 and θ,ϕ, respectively. The function $G_s^r(\mathbf{n},\mathbf{n}_0;t)$ is looked for as a solution of the rotational diffusion equation [37]

$$\frac{\partial G_s^r}{\partial t}=D_r\left[\frac{\partial^2 G_s^r}{\partial\theta^2}+\cot\theta\frac{\partial G_s^r}{\partial\theta}+\frac{1}{\sin^2\theta}\frac{\partial^2 G_s^r}{\partial\phi^2}\right] \qquad (16)$$

with the initial condition

$$G_s^r(\mathbf{n},\mathbf{n}_0;0)=\delta(\mathbf{n}-\mathbf{n}_0). \qquad (17)$$

The probability of all possible events equals unity, therefore the probability density is normalized as

$$\int_0^\pi \sin\theta d\theta\int_0^{2\pi} d\phi G_s^r(\mathbf{n},\mathbf{n}_0;t)=1. \qquad (18)$$

Let us introduce one more frame x', y', z' with the corresponding basis unit vectors $\mathbf{e}'_1,\mathbf{e}'_2,\mathbf{e}'_3$, whose vector $\mathbf{e}'_3$ coincides with $\mathbf{n}_0$. The orientation of the vector $\mathbf{n}$ in this frame is determined by the spherical angles ϑ,φ. It is convenient also to introduce the deviation vector $\Delta\mathbf{n}=\mathbf{n}-\mathbf{n}_0$. As $\vartheta<<1$ it lies in the plane $x'y'$ and its modulus $|\Delta\mathbf{n}|\approx\vartheta$. In such small-angle approximation, Eq. (16) takes the form

$$\frac{\partial G_s^r}{\partial t}=D_r\left[\frac{\partial^2 G_s^r}{\partial\vartheta^2}+\frac{1}{\vartheta}\frac{\partial G_s^r}{\partial\vartheta}+\frac{1}{\vartheta^2}\frac{\partial^2 G_s^r}{\partial\varphi^2}\right], \qquad (19)$$

which coincides with the equation, which describes the translational diffusion of the particle on the plane, written in polar coordinates. The latter includes the radial coordinate ϑ, varying from 0 to ∞ [1], and the azimuth angle φ, varying from 0 to 2π. Hence, a solution of Eq. (19), satisfying the constraints (17) and (18), is

$$G_s^r(\mathbf{n},\mathbf{n}_0;t)=\frac{1}{4\pi D_r|t|}\exp\left(-\frac{\vartheta^2}{4D_r|t|}\right). \qquad (20)$$

Instead of the polar coordinates, ϑ,φ one can employ the Cartesian variables ϑ_1 and ϑ_2, which denote the rotation angles around the vectors $\mathbf{e}'_1$ and $\mathbf{e}'_2$, respectively. Then $\vartheta^2=\vartheta_1^2+\vartheta_2^2$ and the expression (20) becomes

$$G_s^r(\mathbf{n},\mathbf{n}_0;t)=\frac{1}{4\pi D_r|t|}\exp\left(-\frac{\vartheta_1^2+\vartheta_2^2}{4D_r|t|}\right), \qquad (21)$$

where the angles ϑ_i vary from $-\infty$ to ∞. Calculating the mean-square rotation angle $\Delta_r^2\equiv\langle\vartheta_i^2\rangle$ with the aid of Eq. (21), we arrive at Einstein's formula (13), which confirms the correctness of our theory.

In order to find the Fourier transform of $G_s^r(\mathbf{n},\mathbf{n}_0;t)$ we express the components n_x, n_y, n_z of the unit vector $\mathbf{n}$ in spherical angles:

$$n_x=\sin\theta\cos\phi,\quad n_y=\sin\theta\sin\phi,\quad n_z=\cos\theta. \qquad (22)$$

Simple calculations give

$$\vartheta^2=(\Delta\mathbf{n})^2=(\theta-\theta_0)^2+\sin^2\theta_0(\varphi-\varphi_0)^2 \qquad (23)$$

and

$$\boldsymbol{\kappa}(\mathbf{r}-\mathbf{r}_0)=\kappa r\sin\theta_0(\theta-\theta_0). \qquad (24)$$

Applying (23), we transform the rotational correlation function (20) to

$$G_s^r(\mathbf{n},\mathbf{n}_0;t)=\frac{1}{4\pi D_r|t|}\times$$

$$\times\exp\left(-\frac{(\theta-\theta_0)^2}{4D_r|t|}\right)\exp\left(-\frac{\sin^2\theta_0(\phi-\phi_0)^2}{4D_r|t|}\right). \qquad (25)$$

Then by inserting (24) and (25) into (15) one obtains

$$G_s^r(\boldsymbol{\kappa},t)=\exp\left[-\kappa^2 D_r r^2\sin^2\theta_0|t|\right]. \qquad (26)$$

3.3. Magnetization relaxations

Following Ref. [35] we suppose that there is an electric field gradient along the magnetic field $\mathbf{h}_0$ at the nucleus ^{57}Fe. The constant field $\mathbf{h}_0$ gives rise to Zeeman splitting of sublevels $1/2, M_g$ and $3/2, M_e$ of the ground and excited nuclear states, respectively. Here M_g and M_e are the projections of the nuclear spin on the direction $\mathbf{h}_0$. In the fluctuating

[1] In the small-angle approximation the upper border π for ϑ may be replaced by ∞.

field $\mathbf{h}_0(t)$ the Mössbauer spectrum is described by the correlator $G_N(\boldsymbol{\kappa},t)$ [35]

$$G_N(\boldsymbol{\kappa},t)=\sum_{j=1}^{6}J_j(\beta)\exp[-iQ(3M_e^2-15/4)t/\hbar]\times$$

$$\times\left(\exp\left[i\alpha_j\int_0^t f(t')dt'\right]\right)_{av}, \qquad (27)$$

where $(...)_{av}$ implies the stochastic averaging, $f(t)=\pm 1$, the parameter Q determines a quadrupole shift of the lines, the factors $J_{j=M_g\to M_e}(\beta)$ are relative intensities of the Zeeman sextet:

$$J_{1=-1/2\to-3/2}(\beta)=J_{6=1/2\to3/2}(\beta)=\frac{3}{16}(1+\cos^2\beta),$$

$$J_{2=-1/2\to-1/2}(\beta)=J_{5=1/2\to1/2}(\beta)=\frac{1}{4}\sin^2\beta, \qquad (28)$$

$$J_{3=-1/2\to1/2}(\beta)=J_{4=1/2\to-1/2}(\beta)=\frac{1}{16}(1+\cos^2\beta),$$

depending on the angle β between the wave vector of γ-quanta $\boldsymbol{\kappa}$ and magnetization $+\mathbf{M}$. Here the lines of the Zeeman sextet are enumerated in the order of growing energy. In the absence of external magnetic fields, when the particles are oriented randomly, the averaged relative intensities of the lines $J_i=\bar{J}_i(\beta)$ are

$$J_1=J_6=\frac{1}{4},\quad J_2=J_5=\frac{1}{6},\quad J_3=J_4=\frac{1}{12}. \qquad (29)$$

Then the stochastic averaging results in [35]

$$\left(\exp\left[i\alpha_j\int_0^t f(t')dt'\right]\right)_{av}=$$

$$=(\cos x_j wt+x_j^{-1}\sin x_j wt)\exp(-wt), \qquad (30)$$

with parameters

$$x_j=[(\alpha_j/w)^2-1]^{1/2},$$

$$\alpha_j=\alpha_{eg}=(g_gM_g-g_eM_e)\mu_N h_0/\hbar, \qquad (31)$$

depending on the nuclear magneton μ_N and gyromagnetic ratios g_g, g_e of the ground and excited states, respectively. From now on, for brevity, we shall omit the exponential in Eq. (27), associated with the quadrupole splitting. Once $Q\neq 0$, in all equations below the Doppler shift s should be replaced by $s-Q(3M_e^2-15/4)$. In addition, the isomer shift is assumed to be zero.

4. Absorption cross-section

Substituting (9), (26), and (30) into (6) one finds the absorption cross-section

$$\sigma_a(s)=\frac{\sigma_0\Gamma_a}{4}e^{-2W_a}\,Re\sum_{j=1}^{6}J_j\times$$

$$[\left(1-\frac{i}{x_j}\right)\frac{i}{s+x_j\hbar w+i\Gamma_{eff}/2} \qquad (32)$$

$$+\left(1+\frac{i}{x_j}\right)\frac{i}{s-x_j\hbar w+i\Gamma_{eff}/2}].$$

It has an effective width

$$\Gamma_{eff}=\Gamma+\Delta\Gamma_r+\Delta\Gamma_N, \qquad (33)$$

where Γ is defined by Eq. (10), the broadening due to Néel's relaxations $\Delta\Gamma_N=2\hbar w$, the rotational broadening, depending on the coordinates of the Mössbauer nucleus ^{57}Fe,

$$\Delta\Gamma_r\equiv\Delta\Gamma_r(\mathbf{r})=2\hbar\kappa^2D_r r^2\sin^2\theta_0. \qquad (34)$$

When the Brownian broadenings $\Delta\Gamma_t=\Delta\Gamma_r=0$ our Eq. (32) differs from the corresponding result of Ref. [35] only in some unessential details.

For uniform distribution of these nuclei in nanoparticles the averaged cross-section is defined by

$$\langle\sigma_a(s)\rangle=\frac{3}{2a_c^3}\int_0^{a_c}r^2dr\int_0^{\pi}\sigma_a(s)\sin\theta_0 d\theta_0. \qquad (35)$$

Having substituted here the expression (32) we introduce new variables $\xi=\cos\theta_0$ and $\rho=r/a_c$ to obtain

$$\langle\sigma_a(s)\rangle=\frac{3\sigma_0\Gamma_a}{4}e^{-2W}\,Re\sum_{j=1}^{6}J_j\int_0^1\rho^2d\rho\times$$

$$\times\left[\left(1-\frac{i}{x_j}\right)I_j^+(\rho)+\left(1+\frac{i}{x_j}\right)I_j^-(\rho)\right], \qquad (36)$$

where $I_j^{\pm}(\rho)$ stands for the integral

$$I_j^{\pm}(\rho)=\int_0^1\frac{d\xi}{A_j^{\pm}(\rho)-B(\rho)\xi^2} \qquad (37)$$

with

$$B = i\hbar\kappa^2 D_r a_c^2 \rho^2 = (3i/8)\Delta\Gamma_t (a_c/a_h)^2 \rho^2 \quad (38)$$

and

$$A_j^{\pm} = s \pm x_j w + i(\Gamma + \Delta\Gamma_N)/2 + B. \quad (39)$$

Trivial integration gives

$$I_j^{\pm}(\rho) = \frac{1}{\sqrt{A_j^{\pm} B}} Arth\left(\sqrt{B/A_j^{\pm}}\right). \quad (40)$$

In the case of slow relaxations, when $w << |\alpha_j|$ and respectively $x_j >> 1$ as well as $x_j w \approx \alpha_j$, the cross-section reduces to Zeeman's pattern with broadened lines:

$$\langle\sigma_a(s)\rangle = \frac{\sigma_0\Gamma_a}{2} e^{-2W_a} Re \sum_{j=1}^{6} J_j \times$$

$$\times \int_0^1 \rho^2 d\rho \frac{1}{\sqrt{A_j B}} Arth\left(\sqrt{B/A_j}\right), \quad (41)$$

where B is again determined by the formula (38), while A_j taking the form

$$A_j = s - \hbar\alpha_j + i(\Gamma + \Delta\Gamma_N)/2 + B. \quad (42)$$

In the opposite limit of very rapid relaxations as $w >> |\alpha_j|$ the nucleus only feels an average zero magnetic field. In this case, the cross-section collapses to a single line [2]

$$\langle\sigma_a(s)\rangle = \frac{3\sigma_0\Gamma_a}{2} e^{-2W_a} Re \int_0^1 \rho^2 d\rho \times$$

$$\times \frac{1}{\sqrt{AB}} Arth\left(\sqrt{B/A}\right), \quad (43)$$

where B remains the same, while A becomes

$$A = s + i\Gamma/2 + B. \quad (44)$$

Note also that the same expression (43) describes the Mössbauer spectra of nonmagnetic Brownian particles.

The formulas considerably simplify, if we average only $\Delta\Gamma_r(r)$ instead of the whole cross-section (32). Then

$$\langle r^2 \sin^2\theta_0\rangle = 0.4 a_c^2. \quad (45)$$

[2] If $Q \neq 0$ the spectrum collapses to a quadrupole doublet.

In this case, the averaged cross-section is determined by the same general formula (33) but with the rotational broadening $\Delta\Gamma_r$ replaced by

$$\langle\Delta\Gamma_r\rangle = 0.4\hbar\kappa^2 D_r a_c^2 = 0.3\Delta\Gamma_t (a_c/a_h)^2. \quad (46)$$

If the magnetization relaxations are slow the average cross-section becomes

$$\langle\sigma_a(s)\rangle = \frac{\sigma_0\Gamma_a}{4} e^{-2W_a} \sum_{j=1}^{6} J_j \frac{\langle\Gamma_{eff}\rangle}{(s-s_j)^2 + \langle\Gamma_{eff}\rangle^2/4}, \quad (47)$$

where $s_j = \hbar\alpha_j$ defines position of the jth line and the averaged effective width is

$$\langle\Gamma_{eff}\rangle = \Gamma + \Delta\Gamma_N + \langle\Delta\Gamma_r\rangle. \quad (48)$$

In the regime of fast relaxations

$$\langle\sigma_a(s)\rangle = \frac{\sigma_0\Gamma_a}{4} e^{-2W_a} \frac{\Gamma + \langle\Delta\Gamma_r\rangle}{s^2 + (\Gamma + \langle\Delta\Gamma_r\rangle)^2/4}. \quad (49)$$

If the contribution of rotation is neglected, Eq. (49) coincides with the result of Singwi and Sjolander [25].

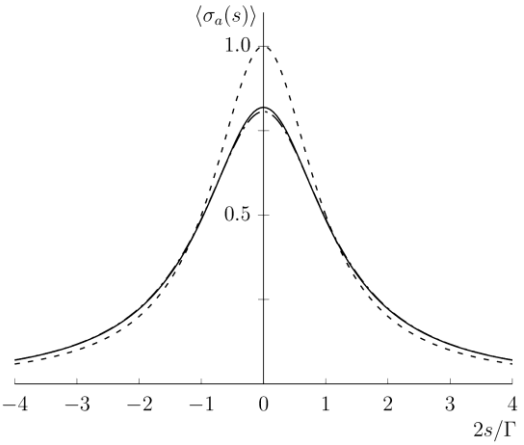

Fig. 2. Dependence of the absorption cross-sections on the Doppler shift s, expressed in units $\Gamma/2$. The cross-section calculated by Eq. (43) is drawn by the solid line, the result of Singwi and Sjolander [25] by dashed one, the approximate expression (47) by dash-dotted.

The role of rotational diffusion is illustrated in Fig. 2, where all the cross-sections are calculated in units $(\sigma_0\Gamma_a/\Gamma)e^{-2W_a}$ as a function of the dimensionless parameter $2s/\Gamma$ for the case, when $\Gamma = \Gamma_0 + \Delta\Gamma_t = 5\Gamma_0$ and $a_c = a_h$. The exact cross-section (43) is drawn by the solid line. The Singwi-Sjolander's curve, given by Eq. (49) with $\langle\Delta\Gamma_r(\mathbf{r})\rangle = 0$, by the dashed one. For comparison, the approximate curve (49) is shown by the dash-dotted line, calculated with the aid of Eq. (46). It is

seen that it surprisingly well approximates the exact result (43).

5. Approach based on Langevin's equation

The correlation function (8) is not valid at small times. More correctly self-diffusion is described by the correlation function [25, 38]

$$G_s^t(\mathbf{R},t) = [2\pi\rho_t(t)]^{-3/2}\exp\left[-\frac{R^2}{2\rho_t(t)}\right], \quad (50)$$

where

$$\rho_t(t) = \frac{2D_t}{\beta_t}\left[\beta_t t - 1 + \exp(-\beta_t t)\right] \quad (51)$$

with

$$\beta_t = 6\pi a\eta / m = \frac{kT}{D_t m}. \quad (52)$$

The parameter β_t^{-1} means the characteristic (relaxation) time for the Brownian translational motion of the particle with mass m.

At $t >> \beta_t^{-1}$ the correlation functions (8) and (50) coincide. In the opposite limit as $t << \beta_t^{-1}$ the diffusion approach leads to a paradox, remarked in Ref. [32]. Then the mean-square displacement $\langle x^2\rangle = 2D_t t$, and therefore the root-mean-square velocity along the axis x, given by $\sqrt{\langle v_x^2\rangle} = \sqrt{2D_t / t}$, diverges as t approaches zero. However, from the more correct correlation function (51), (52) it follows that at $t << \beta_t^{-1}$ the mean-square displacement $\langle x^2\rangle = D_t\beta_t t^2$, hence $\sqrt{\langle v_x^2\rangle} = \sqrt{D_t\beta_t} = (kT/m)^{1/2}$. Thus, the mean kinetic energy of the Brownian particle $\bar{E}_{kin}$ at $t \to 0$ occurs to be determined by the same expression as $\bar{E}_{kin}$ for the molecules of the ideal gas:

$$\bar{E}_{kin} = 3kT/2. \quad (53)$$

The function (50) was derived by Chandrasekhar [38] from Langevin's equation

$$\frac{d^2\mathbf{R}}{dt^2} = -\beta_t\frac{d\mathbf{R}}{dt} + \mathbf{F}_{rand}(t)/m. \quad (54)$$

Here on the right-hand side, the first term stands for the friction force over mass, $\mathbf{F}_{rand}(t)$ for random forces acting on the Brownian particle.

Let us find now the rotational correlation function, analogous to (50), starting from the well-known relationship between the angular momentum $\mathbf{L}$ of the rotating rigid body and the total torque $\mathbf{K}$ acting on it [39]:

$$\frac{d\mathbf{L}}{dt} = \mathbf{K}. \quad (55)$$

In the case considered the $\mathbf{K}$ equals a sum of the friction torque [40]

$$\mathbf{K}_{fr} = -8\pi\eta a_h^3\boldsymbol{\omega}. \quad (56)$$

and torques $\mathbf{K}_{rand}(t)$ due to random forces.

We take into account that the angular momentum for a rigid sphere of the radius a is related to its angular frequency of rotation $\boldsymbol{\omega}$ by

$$\mathbf{L} = I\boldsymbol{\omega}, \quad (57)$$

where the inertia moment of the rigid sphere

$$I = 0.4ma_h^2. \quad (58)$$

Inserting (56), (57) into (55) one gets the equation, governing the stochastic rotational motion:

$$\frac{d\boldsymbol{\omega}}{dt} = -\beta_r\boldsymbol{\omega} + \mathbf{K}_{rand}(t)/I, \quad (59)$$

where

$$\beta_r = \frac{20\pi\eta a_h}{m} = \frac{5}{2}\frac{kT}{D_r m a_h^2}. \quad (60)$$

Keeping in mind that the components of the angular velocity $\boldsymbol{\omega}$ along the vectors $\mathbf{e}'_i$ are defined as $\omega_i = d\vartheta_i / dt$ we transform (59) to the equation

$$\frac{d^2\vartheta_i}{dt^2} = -\beta_r\frac{d\vartheta_i}{dt} + K_{rand}(t)/I, \quad (61)$$

formally equivalent to Langevin's equation (54) in a two-dimensional case. Here in the same approximation we ignore the boundary conditions for the angle ϑ_i and accept that it ranges from $-\infty$ to ∞. Further repeating derivation, done by Chandrasekhar [36], one gets the correlation function

$$G_s^r(\vartheta,t) = \frac{1}{2\pi\rho_r(t)}\exp\left[-\frac{\vartheta^2}{2\rho_r(t)}\right], \quad (62)$$

where the function $\rho_r(t)$ is again defined by Eq. (51), but with index t replaced by r. As to the Fourier-transform, it is given now by

$$G_s^r(\boldsymbol{\kappa},t) = \exp\left[-\kappa^2\rho_r(t)r^2\sin^2\theta_0/2\right]. \quad (63)$$

Combining these equations we get in the slow-relaxation limit the cross-section as a superposition of six lines:

$$\sigma_a(s) = \sum_{j=1}^{6} \sigma_a^{(j)}(s), \qquad (64)$$

each of them is given by

$$\sigma_a^{(j)}(s) = \frac{\sigma_0 \Gamma_a}{4} e^{-2W_a} e^{b_t + b_r} J_j \times$$

$$\times \sum_{n,k=0}^{\infty} \frac{(-b_t)^n}{n!} \frac{(-b_r)^k}{k!} \frac{\Gamma_{n,k}}{(s - s_j)^2 + \left(\frac{\Gamma_{n,k}}{2}\right)^2}, \qquad (65)$$

where we introduced the parameters

$$b_t = \frac{\kappa^2 D_t}{\beta_t}, \qquad b_r = \frac{\kappa^2 D_r r^2 \sin^2\theta_0}{\beta_r} \qquad (66)$$

and the widths

$$\Gamma_{n,k} = \Gamma_{eff} + 2n\hbar\beta_t + 2k\hbar\beta_r. \qquad (67)$$

Again we replace averaging of the cross-section over the uniform distribution of Mössbauer nuclei inside the particle by averaging $r^2 \sin^2\theta_0$ i.e., this product is replaced by $\langle r^2 \sin^2\theta_0 \rangle = 0.4 a_c^2$. Then one has a relation

$$\langle b_r(r) \rangle = 0.045 b_t, \qquad (68)$$

which allows to set in (65) $b_r \approx 0$.

The integral width of the *j*-th Zeeman line is determined by the formula

$$\Gamma_{int} = \frac{2}{\pi \sigma_a^{(j)}(s_j)} \int_{-\infty}^{\infty} \sigma_a^{(j)}(s) ds. \qquad (69)$$

Here

$$\int_{-\infty}^{\infty} \sigma_a(s) ds = \frac{\pi}{2} \sigma_0 \Gamma_a e^{-2W_a}. \qquad (70)$$

Therefore

$$\Gamma_{int} = e^{-b_t} \left[\sum_{n=0}^{\infty} \frac{(-1)^n}{n!} \frac{(b_t)^n}{\langle \Gamma_n \rangle} \right]^{-1}, \qquad (71)$$

where the width $\langle \Gamma_n \rangle = \langle \Gamma_{eff} \rangle + 2n\hbar\beta_t$ and the average effective width are determined by Eq. (48).

The significance of Langevin's approach is illustrated in Fig. 3, where the Brownian broadening $\langle \Delta\Gamma_B \rangle$ for magnetite MNPs with a diameter of 700 nm is calculated by Eq. (46) (curve *1*) and by Eq. (71) (curve *2*). In the last case, we put $b_r = 0$, so that the translational Brownian motion is described by Langevin's equation and the rotational one by simple diffusion equation. Note that in previous articles [23, 24] the Brownian rotation has not been taken into consideration at all.

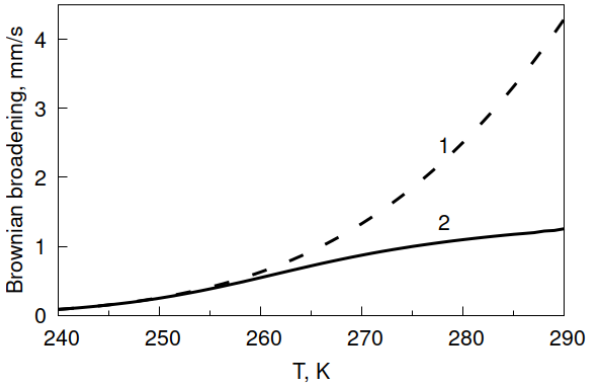

Fig. 3. Brownian broadening of the absorption lines vs temperature for the magnetite nanoparticles with radius $a_h = a_c = 350$ nm in the 60 % glycerol-water mixture, calculated in the diffusion approach (*1*) and Langevin's one (*2*).

6. Discussion

We have derived the expression (32) for the absorption cross-section $\sigma_a(s)$ of Mössbauer radiation by a single nucleus ^{57}Fe, whose position inside the MNP is determined by the radius vector **r**. All the relaxation mechanisms are taken into consideration – Néel's relaxations of the particle magnetization as well as the Brownian translational and rotational motion, which ensure the broadenings of the Mössbauer lines $\Delta\Gamma_N$, $\Delta\Gamma_t$ and $\Delta\Gamma_r(\mathbf{r})$, respectively. Assuming the uniform distribution of the Mössbauer nuclei inside the MNP, we got rather cumbersome Eqs. (36) - (44) for the average cross-section $\langle \sigma_a(s) \rangle$. The situation is significantly simplified by averaging only the $\Delta\Gamma_r$ instead of $\sigma_a(s)$. As is seen from Fig. 2, the cross-section (47), calculated in this approximation, is very close to the exact cross-section (36).

Dependence $\Delta\Gamma_t$ on temperature for large Brownian particles is well described by means of the correlation function, which is obtained from the stochastic Langevin equation [23, 24]. So far nothing like this has been done for the rotational Brownian motion. Therefore for Brownian rotation, we derived Eq. (61) similar to Langevin's equation and suggested the corresponding correlation function (62). In the framework of Langevin's approach to both translational and rotational motion, we obtained a general expression (65) for the cross-section. It occurred that the Langevin rotational corrections to the cross-section are much weaker than the translational ones. Therefore curve *2* in Fig. 3 is calculated by describing the translational motion by Langevin's equation and the rotational one by the diffusion equation.

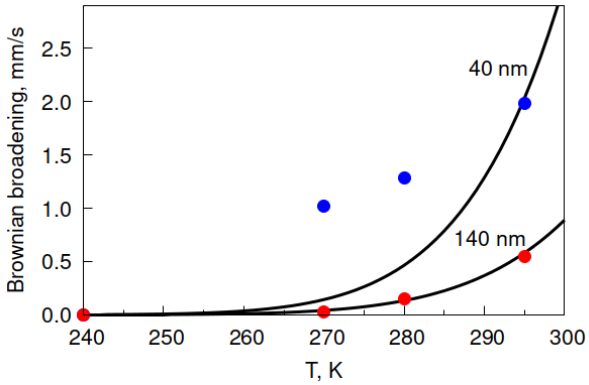

Fig. 4. Brownian broadening of the absorption lines vs temperature for the magnetite nanoparticles with diameters 40 nm and 140 nm dissolved in 96 % glycerol-water mixture. The experiment [33] is presented by circles, our calculations by solid curves. (See color Figure on the journal website.)

In Fig. 4 our calculations are compared with the experimental data of Cherepanov et al. [34]. From the Mössbauer spectra of ferrofluids, they subtracted the spectra of dried samples, which enabled them to extract the contribution only of the Brownian motion into the broadening of the spectral lines. The calculated dependence of the Brownian broadening $\Delta\Gamma_t + \langle \Delta\Gamma_r \rangle$ on temperature is presented in Fig. 4 by solid lines and the experimental data by circles. The calculations very well agree with the experiment for large particles having a diameter of 140 nm, while they terribly diverge for small MNPs with $2a_c = 40$ nm. The reason for such contradiction remained unclear.

REFERENCES

1. R.E. Rosensweig. *Ferrohydrodynamics* (Cambridge, London: Cambridge Univ. Press, 1985); republished (New York: Dover. Publ. Inc., 1997).
2. B.M. Berkovski, V. Bashtovoy. *Magnetic Fluids and Applications Handbook* (New York: Begell House Inc., 1996).
3. C. Scherer, A.M. Figueiredo Neto. Ferrofluids: properties and applications. Brazil. J. Phys. 35 (2005) 718.
4. D.H. Wang, W.H. Liao. Magnetorheological fluid dampers: A review of parametric modelling. Smart Mater. Struct. 20 (2011) 023001.
5. K. Ray, R. Moskowitz. Commercial applications of ferrofluids. J. Magn. Magn. Mater. 85 (1990) 233.
6. K. Ray, R. Moskowitz, R. Casciari. Advances in ferrofluid technology. J. Magn. Magn. Mater. 149 (1995) 174.
7. R. Pérez-Castillejos et al. The use of ferrofluids in micromechanics. Sens. Actuators A 84 (2000) 176.
8. E.H. Kim et al. Synthesis of ferrofluid with magnetic nanoparticles by sonochemical method for MRI contrast agent. J. Magn. Magn. Mater. 289 (2005) 328.
9. V.V. Mody, A. Singh, B. Wesley. Basics of magnetic nanoparticles for their application in the field of magnetic fluid hyperthermia. Eur. J. Nanomed. 5 (2013) 11.
10. K.M. Krishnan. Magnetic nanoparticles in medicine: progress, problems, and advances. IEEE Trans. Magn. 46 (2019) 2523.
11. B. Gleich, J. Weizenecker. Tomographic imaging using the nonlinear response of magnetic particles. Nature 435 (2005) 1214.
12. R.M. Ferguson et al. Optimizing magnetite nanoparticles for mass sensitivity in magnetic particle imaging. Med. Phys. 38 (2011) 1619.
13. R.J. Deissler, Y. Wu, M.A. Martens. Dependence of Brownian and Néel relaxation times on magnetic field strength. Med. Phys. 41 (2014) 012301.
14. Y. Xiao, J. Du. Superparamagnetic nanoparticles for biomedical applications. J. Mater. Chem. B 8 (2020) 354.
15. H.T.K. Duong et al. A guide to the design of magnetic particle imaging tracers for biomedical applications. Nanoscale 14 (2022) 3890.
16. L. Néel. Théorie du traînage magnétique des ferromagnétiques en grains fins avec application aux terres cuites. Ann. Geophys. 5 (1949) 99.
17. J. Landers et al. Simultaneous study of Brownian and Néel relaxation phenomena in ferrofluids by Mössbauer spectroscopy. Nano Lett. 16 (2016) 1150.
18. P.P. Craig, N. Sutin. Mössbauer effect in liquids: influence of diffusion broadening. Phys. Rev. Lett. 11 (1963) 460.
19. D.St.P. Bunbury et al. Study of diffusion in glycerol by the Mössbauer effect of Fe^{57}. Phys. Lett. 6 (1963) 34.
20. T. Bonchev et al. A study of Brownian motion by means of the Mössbauer effect. Sov. Phys. JETP 23 (1966) 42.
21. K.P. Singh, J.G. Mullen. Mössbauer study of Brownian motion in liquids: colloidal cobaltous hydroxy stannate in glycerol, ethanol-glycerol, and aqueous-glycerol solutions. Phys. Rev. A 6 (1972) 2354.
22. V.N. Dubinin. Influence of viscosity of colloidal solutions on the magnitude of resonance absorption of γ-quanta. Ukr. J. Phys. 13 (1968) 1547. (Rus)
23. S.L. Kordyuk et al. Mössbauer effect in a disperse system. Sov. Phys. JETP 25 (1967) 400.
24. V.G. Bhide et al. Effect of Brownian motion on the Mössbauer line shape. Phys. Rev. B 3 (1971) 673.
25. K.S. Singwi, A. Sjölander. Resonance absorption of nuclear gamma rays and the dynamics of atomic motions. Phys. Rev. 120 (1960) 1093.
26. A.V. Zatovski. Contribution to the theory of the Mössbauer effect on Brownian particles. Sov. Phys. JETP 32 (1971) 274.
27. O.Ya. Dzyublik. On the theory of the Mössbauer effect on Brownian particles. Ukr. J. Phys. 18 (1973) 1454. (Ukr)
28. A.Ya. Dzyublik. Mössbauer effect in ellipsoidal Brownian particles. Sov. Phys. JETP 40 (1975) 763.

29. A.M. Afanas'ev, P.V. Hendriksen, S. Mørup. Influence of rotational diffusion of the Mössbauer spectrum of ultrafine particles in a supercooled liquid. Hyperf. Inter. 88 (1994) 35.
30. А.Я. Дзюблик. Теория эффекта Мессбауэра на магнитных броуновских частицах. УФЖ 23 (1978) 881. / A.Ya. Dziublik. Theory of the Mössbauer effect on magnetic Brownian particles. Ukr. J. Phys. 23 (1978) 881.
31. J. Landers et al. In-field orientation and dynamics of ferrofluids studied by Mössbauer spectroscopy. ACS Appl. Mater. Interfaces 11 (2018) 3160.
32. M.A. Chuev et al. Separation of contributions of the magnetic relaxation and diffusion of nanoparticles in ferrofluids by analyzing the hyperfine structure of Mössbauer spectra. JETP Lett. 108 (2018) 59.
33. R. Gabbasov et al. Study of Brownian motion of magnetic nanoparticles in viscous media by Mössbauer spectroscopy. J. Magn. Magn. Mater. 475 (2019) 146.
34. V.M. Cherepanov et al. Study of the Brownian broadening in the Mössbauer spectra of magnetic nanoparticles in colloids with different viscosities. Crystal. Rep. 65 (2020) 398.
35. M. Blume, J.A. Tjon. Mössbauer spectra in a fluctuating environment. Phys. Rev. 165 (1968) 446.
36. A. Einstein. Zur Theorie der Brownschen Bewegung. Ann. Phys. 19 (1906) 371.
37. M.A. Leontovich. *Introduction to Thermodynamics. Statistical Physics* (Moskva: Vysshaya shkola, 1983). (Rus)
38. S. Chandrasekhar. Stochastic problems in physics and astronomy. Rev. Mod. Phys. 15 (1943) 1.
39. L.D. Landau, E.M. Lifshitz. *Mechanics*. 3d edition (Oxford: Elsevier Ltd, 1976).
40. G. Kirchhoff. *Vorlesungen über Mechanik* (Leipzig: B.G. Teubner, 1897).

О. Я. Дзюблик*, І. Є. Анохін, В. Ю. Співак

Інститут ядерних досліджень НАН України, Київ, Україна

*Відповідальний автор: dzyublik@ukr.net

РОЛЬ БРОУНІВСЬКОГО РУХУ ТА РЕЛАКСАЦІЙ НЕЄЛЯ У МЕССБАУЕРІВСЬКИХ СПЕКТРАХ МАГНІТНИХ РІДИН

Розраховано переріз поглинання мессбауерівського випромінювання в магнітних рідинах з урахуванням як поступального, так і обертального броунівського рухів магнітних наночастинок, а також стохастичних інверсій їх намагніченості за відсутності зовнішнього магнітного поля. Роль броунівського руху у ферорідинах розглядається в рамках теорії дифузії, а для магнітореологічних рідин з великими наночастинками – за допомогою підходу Ланжевена. Для стохастичного обертання ми вивели рівняння, аналогічне рівнянню Ланжевена, і знайшли відповідну кореляційну функцію. В обох випадках прості обертальні кореляційні функції отримано в наближенні малих обертів за час життя збуджених мессбауерівських ядер. Вплив релаксацій Неєля розглядається в рамках моделі Блюма.

Ключові слова: ефект Мессбауера, феромагнітні наночастинки, броунівський рух, релаксації Неєля.

Надійшла / Received 23.05.2024